Spectral analysis for the iron-based superconductors: Anisotropic spin fluctuations and fully gapped $s^{\pm}$-wave superconductivity

Junhua Zhang[1], Rastko Sknepnek[1,2], and Jörg Schmalian[1]

[1]*Department of Physics and Astronomy and Ames Laboratory, Iowa State University, Ames, IA 50011, USA*
[2]*Department of Materials Science and Engineering Northwestern University, Evanston, IL 60208, USA*
(Dated: October 25, 2010)

Spin fluctuations are considered to be one of the candidates that drive a sign-reversed $s^{\pm}$ superconducting state in the iron pnictides. In the magnetic scenario, whether the spin fluctuation spectrum exhibits certain unique fine structures is an interesting aspect for theoretical study in order to understand experimental observations. We investigate the detailed momentum dependence of the short-range spin fluctuations using a 2-orbital model in the self-consistent fluctuation exchange approximation and find that a common feature of those fluctuations that are capable of inducing a fully gapped $s^{\pm}$ state is the momentum anisotropy with lengthened span along the direction transverse to the antiferromagnetic momentum transfer. Performing a qualitative analysis based on the orbital character and the deviation from perfect nesting of the electronic structure for the 2-orbital and a more complete 5-orbital model, we gain the insight that this type of anisotropic spin fluctuations favor superconductivity due to their enhancement of intra-orbital, but inter-band, pair scattering processes. The momentum anisotropy leads to elliptically shaped magnetic responses which have been observed in inelastic neutron scattering measurements. Meanwhile, our detailed study on the magnetic and the electronic spectrum shows that the dispersion of the magnetic resonance mode in the nearly isotropic $s^{\pm}$ superconducting state exhibits anisotropic propagating behavior in an upward pattern and the coupling of the resonance mode to fermions leads to a dip feature in the spectral function.

I. INTRODUCTION

Since the discovery of the iron-based superconductors,[1] intensive research has been carried out and great progress has been made to understand the microscopic mechanism of superconductivity and the interplay between superconducting (SC), magnetic and structural transitions. Still, many issues remain unclear such as the the pairing mechanism, pairing symmetry, gap structure and the nature of the magnetism. As the electron-phonon coupling seems to be inadequate to account for the relatively high transition temperatures,[2] electronic interactions will likely play a role in the pair formation. Based on the experience in high temperature cuprates, organic superconductors, and heavy fermion superconductors with their commonality of proximity to magnetism, comparative analyses have been made to show the similarities and differences between different classes of superconductors.[3] This directs the attention to the long discussed magnetic pairing mechanism.[4] Renormalization group studies[5,6] on the iron pnictides show that the underlying electronic structure, when close to perfect nesting, develops an unconventional pairing interaction enabled by interband pair-hopping and further amplified by antiferromagnetic correlations. Therefore electronic and magnetic fluctuations, which are active in the vicinity of magnetic transition, have been listed as one of the candidates to mediate Cooper pairs in the material.[5–10] The pairing symmetry and gap structure are among the most interesting topics as they contain most relevant information on pairing mechanism. However there is no consensus on them when explored using different experimental methods and in different members of the material. Further, although being

considered as layered structure, the material should be considered anisotropic, but three dimensional. Some evidence shows gap nodes along the c-axis.[11] Even for the in-plane gap structure, some experiments support fully gapped structure and some indicate in-plane gap nodes. Theoretical explorations suggest the strongest pairing instability corresponds to the sign-reversed $s^{\pm}$-wave state, without ruling out other forms like d-wave and conventional s-wave. Even in the sign-reversed $s^{\pm}$ state, depending on detailed Fermi surface (FS) configuration, different form factors of the Cooper pair could be developed, resulting in either fully gapped $s^{\pm}$-wave spectrum on all FS sheets or nodal $s^{\pm}$-wave with sign change on the electron pockets.[12–14] Besides, associated with the multiband character, evidence of multiple gaps is found in some systems. It has been clear that the material is metallic in the parent compound with well-established long range antiferromagnetic (AFM) order. But with noticeable electronic correlations the nature of magnetism is still under debate.

The magnetic excitation spectrum carries important information on the nature of magnetism and the characteristics of superconductivity. For the latter, it has been discussed in the context of cuprates that an observation of a sharp quasiparticle-like resonance peak in the spin fluctuation spectrum with the onset of superconductivity may strongly indicate a sign change in the gap structure due to the superconducting coherence factors. And the analogous discussion has been applied to the iron pnictides[15–18] based on the random phase approximation and the mean-field BCS approximation, showing that a strong spin resonance occurs in the $s^{\pm}$-wave SC state. This indicates that the spin resonance phe-

nomenon is compatible with the $s^{\pm}$-wave SC gap. Meanwhile, as a momentum resolved probe of the spin correlation, inelastic neutron scattering (INS) experiments have reported the observation of resonance mode in both hole-doped and electron-doped 122 system[19–22] as well as in the $FeTe_{1-x}Se_x$ system.[23,24] Notice that the spin resonance is a consequence of the sign-reversed gap opening in the quasiparticle spectrum not an evidence for the magnetic pairing glue. In order to reveal the relationship between AFM fluctuations and superconductivity in the iron-based materials, more detailed inspections on the structure of the spin fluctuations are needed. Recently, INS measurements observe the same type of anisotropic feature in the magnetic spectrum both in the normal and in the SC state of the 122 system.[25–27] This anisotropy is characterized by larger broadening along the transverse direction with respect to the AFM wave vector $\mathbf{Q}_{AFM}$ in momentum space. Ref.[27] also shows no changes observed in the spatial correlations through T_c, which is consistent with the magnetic scenario in that the onset of superconductivity does not change magnetic correlation length. Early theoretical exploration on the short-range spin-fluctuation induced superconductivity has argued that magnetic fluctuations throughout an extended momentum region near AFM wave vector $\mathbf{Q}_{AFM}$ are relevant to superconductivity. Thus it raises a question: is the observed anisotropic feature of the spin fluctuations, i.e., larger broadening along the transverse direction in momentum space, consistent with superconductivity in this system?

On the other hand, as discussed for cuprates,[28–30] an important identification of the mediating boson, if it exists, is from the fermionic spectrum which can be observed by angle-resolved photoemission spectroscopy (ARPES). Indeed, ARPES has reported the observations of kink feature in the electronic dispersion for the hole-doped 122 system.[31–33] However there is discrepancy in its vanishing temperature among the observations from different groups. If it is unique to the SC state, i.e., vanishing above T_c, and the subtracted bosonic mode energy coincides with the resonance energy, it would be a strong evidence for magnetic pairing mechanism.

Motivated by these experimental facts, we perform a detailed investigation of the spin and charge spectra in the normal and superconducting states, in which the magnetic susceptibility and the SC gap function are determined within the self-consistent fluctuation exchange (FLEX) approximation using a 2-orbital model for iron pnictides. This itinerant model calculation finds a fully gapped $s^{\pm}$-wave SC state driven by the enhanced commensurate AFM correlation. Based on a systematic study on the momentum structure of the short-range spin fluctuations, we find the same type of anisotropy as that observed in INS measurements. To understand the interplay between the fluctuation anisotropy and the $s^{\pm}$ superconductivity, we present a qualitative analysis through the orbital contents and the deviation from perfect nesting of the electronic structure for the 2-orbital

and a more complete 5-orbital model. Meanwhile, the calculated dispersion of the magnetic resonance mode exhibits an anisotropic propagating pattern. And the calculated fermionic spectral function shows the fingerprint of electron-mode coupling as observed in ARPES.

II. MODEL

We consider a Hamiltonian described by a 2-orbital tight-binding model and on-site multiorbital electronic interactions,

$$
\begin{aligned}
H = {} & \sum_{\mathbf{k},ab,\sigma} \varepsilon_{\mathbf{k}}^{ab} d_{\mathbf{k}a\sigma}^{\dagger} d_{\mathbf{k}b\sigma} + U \sum_{i,a} n_{ia\uparrow} n_{ia\downarrow} + U' \sum_{i,a>b} n_{ia} n_{ib} \\
& + J_H \sum_{i,a>b,\sigma\sigma'} d_{ia\sigma}^{\dagger} d_{ib\sigma'}^{\dagger} d_{ia\sigma'} d_{ib\sigma} \\
& + J' \sum_{i,a\neq b} d_{ia\uparrow}^{\dagger} d_{ia\downarrow}^{\dagger} d_{ib\downarrow} d_{ib\uparrow}
\end{aligned}
\tag{1}
$$

where $n_{ia\sigma} = d_{ia\sigma}^{\dagger} d_{ia\sigma}$ is the occupation number of the orbital a with spin σ at site i and $n_{ia} = \sum_{\sigma} n_{ia\sigma}$ with the orbital index $a(b)$ standing for the Fe orbitals d_{xz} and d_{yz}. The tight-binding description[34] is given by $\varepsilon_{\mathbf{k}}^{xy} = \varepsilon_{\mathbf{k}}^{yx} = -4t_4 \sin k_x \sin k_y$ and $\varepsilon_{\mathbf{k}}^{aa} = -2t_1 \cos k_a - 2t_2 \cos k_b - 4t_3 \cos k_x \cos k_y - \mu$ where $a, b = x(y)$ stand for $d_{xz}(d_{yz})$ orbitals and the momentum components with $a \neq b$. We use the tight-binding parameters $t_1 = -0.33$, $t_2 = 0.385$, $t_3 = -0.234$, and $t_4 = -0.26$.[35,36] Near half filling this tight-binding model gives rise to the FS that contains two hole pockets and two electron pockets for which we refer to the hole pockets around $(0,0)$ and (π,π) as α_1 and α_2 sheets, respectively, and the electron pockets around $(\pi,0)$ and $(0,\pi)$ as β_1 and β_2 sheets, respectively, in the unfolded (1 Fe per unit cell) Brillouin zone (BZ). As noted by Kuroki *et al.*[37] and Kemper *et al.*[14], the appearance of a hole pocket around the (π,π) point of the unfolded BZ is crucial to the formation of fully gapped $s^{\pm}$ state. The predominant Fe-orbital character distribution on each FS sheet has been analyzed in Ref.[38]. In the 5-orbital tight-binding description,[14] a third orbital d_{xy} predominantly contributes to the hole pocket at the (π,π) point and partially to the $(\pi,0)$ and $(0,\pi)$ electronic pockets. Although the 2-orbital model does not include the third predominant orbital composition on the FS, as we will show later, the intra-orbital nesting configuration of it remains similar to that of the 5-orbital description, which is believed to play an important role for the magnetic fluctuation and the superconductivity in the itinerant picture. Thus this simplified 2-orbital description qualitatively captures the key features of the electronic structure near the Fermi energy, serving as a good starting point for the understanding of the interplay between magnetism and superconductivity in the Fe-based superconductors.

The on-site interactions consist of the intra- and inter-orbital Coulomb repulsions controlled by the coupling

constant U and U', the inter-orbital Hund's rule coupling J_H and pair hopping term J'. For the bare Coulomb interaction, due to rotational symmetry, the coupling constants are related by $U = U' + 2J$ and $J = J_H = J'$. However, as discussed in the Ref.[36], when they are parameters in an approximate theory such as FLEX which ignores vertex corrections, they are not identical to the bare Coulomb matrix elements but should be considered as low energy coupling parameters that have been renormalized by high energy excitations. Therefore we study cases with various parameter values and present the typical results here.

Using FLEX approximation[39] for the SC state[40,41], one self-consistently calculates the single-particle propagators renormalized by interactions due to the exchange of spin and charge/orbital fluctuations and the spin and charge/orbital correlation renormalized by the polarization of dressed quasiparticles. In the SC state, Cooper-pair condensation causes a finite anomalous self-energy, which can be treated as the SC order parameter, and induces a contribution from the anomalous quasiparticle propagator to the fluctuations. In this work we consider only singlet pairing and assume time reversal symmetry in the system.

The complete multiorbital FLEX equations can be found in the Ref.[42]. Here we present only expressions that are relevant to our discussions. The magnetic susceptibility is theoretically calculated using the Matsubara frequency as

$$\chi_s\left(\mathbf{q}, i\nu_n\right) = \sum_{aa,bb} \chi_s^{aa,bb}\left(\mathbf{q}, i\nu_n\right), \quad (2)$$

with bosonic Matsubara frequency $\nu_n = 2n\pi T$ and the orbital-resolved spin susceptibility calculated in the orbital-matrix expression

$$\hat{\chi}_s\left(\mathbf{q}, i\nu_n\right) = \left[\hat{1} - \hat{\chi}_{s,0}\left(\mathbf{q}, i\nu_n\right)\hat{U}_s\right]^{-1} \hat{\chi}_{s,0}\left(\mathbf{q}, i\nu_n\right) (3)$$

where $\hat{U}_s$ is the spin-sector interaction matrix given by $U_s^{aa,aa} = U$, as well as $U_s^{ab,ab} = U'$, $U_s^{ab,ba} = J'$, and $U_s^{aa,bb} = J_H$ if $a \neq b$.[36] Here the bare susceptibility in the superconducting state is calculated as

$$\chi_{s,0}^{ab,a'b'}\left(\mathbf{q}, i\nu_n\right) =$$
$$- \frac{T}{N} \sum_{\mathbf{k},\omega_n}\Big[G^{ba'}\left(\mathbf{k}+\mathbf{q}, i\omega_n+i\nu_n\right)G^{b'a}\left(\mathbf{k}, i\omega_n\right)$$
$$+ F^{bb'}\left(\mathbf{k}+\mathbf{q}, i\omega_n+i\nu_n\right)F^{a'a}\left(\mathbf{k}, -i\omega_n\right)\Big] \quad (4)$$

with the dressed normal and anomalous single-particle propagators determined by solving the coupled Dyson-Gorkov's equations

$$\hat{G}(k) = \hat{G}_0(k) + \hat{G}_0(k)\hat{\Sigma}(k)\hat{G}(k) + \hat{G}_0(k)\hat{\Phi}(k)\hat{F}(k')^*,$$
$$\hat{F}(k) = \hat{G}_0(k)\hat{\Sigma}(k)\hat{F}(k) - \hat{G}_0(k)\hat{\Phi}(k)\hat{G}(k')^*, \quad (5)$$

where $k = (\mathbf{k}, i\omega_n)$, $k' = (-\mathbf{k}, i\omega_n)$ with fermionic Matsubara frequency $\omega_n = (2n+1)\pi T$. The normal and anomalous self-energies

$$\Sigma^{ab}(\mathbf{k}, i\omega_n)$$
$$= \frac{T}{N}\sum_{\mathbf{q},\nu_n}\sum_{m,n}\Gamma_N^{am,bn}(\mathbf{q}, i\nu_n)G^{mn}(\mathbf{k}-\mathbf{q}, i\omega_n-i\nu_n), \quad (6)$$
$$\Phi^{ab}(\mathbf{k}, i\omega_n)$$
$$= \frac{T}{N}\sum_{\mathbf{q},\nu_n}\sum_{m,n}\Gamma_A^{am,nb}(\mathbf{q}, i\nu_n)F^{mn}(\mathbf{k}-\mathbf{q}, i\omega_n-i\nu_n), \quad (7)$$

are related to the renormalized spin and charge/orbital susceptibility through the normal and anomalous interaction vertices $\hat{\Gamma}_N$ and $\hat{\Gamma}_A$.

Carrying out the analytical continuation from Matsubara frequencies to the real frequencies numerically using Padé approximant, the dynamical spin susceptibility is given by

$$\chi_s(\mathbf{q}, \omega) = \chi_s\left(\mathbf{q}, i\nu_n \to \omega + i\delta\right), \quad (8)$$

whose imaginary part $\text{Im}\chi_s$ directly relates to INS intensity. Simultaneously the quasiparticle spectral function is obtained as

$$A(\mathbf{k}, \omega) = -\frac{1}{\pi}\text{Im}\left[\sum_a G^{aa}(\mathbf{k}, i\omega_n \to \omega + i\delta)\right], \quad (9)$$

which corresponds to ARPES intensity.

III. SUPERCONDUCTING GAP STRUCTURE

Within the framework of the self-consistent fluctuation exchange approximation, we search for stable SC solution using the above itinerant model at different coupling constants, doping levels and temperatures. Further we examine the features of the magnetic response for systems that develop superconductivity induced by exchange of short-range fluctuations. In FLEX formalism both spin and charge/orbital fluctuations contribute to the pairing interaction, but the major contribution to the pairing glue comes from spin fluctuations for the parameter regime we are studying. The nested structure of the FS leads to peak in the magnetic susceptibility near the AFM wave vector $\mathbf{Q}_{\text{AFM}} = (0, \pi)$, $(\pi, 0)$, which is strongest at half-filling, $n = 2.0$ per site, indicating its correspondence to the parent compound.

The calculations are performed on imaginary frequency axis for a lattice of 64×64 sites with 8192 Matsubara frequencies. When self-consistently solving the FLEX equations, the convergence of iterations is considered achieved when the maximum relative difference between two consecutive iterations of the self-energy element, $\Sigma^{ab}(\mathbf{k}, i\omega_n)$ or $\Phi^{ab}(\mathbf{k}, i\omega_n)$, is less than 10^{-6}.

For the current model we only find stable SC solutions in the hole doped regime, with the particle density $1.85 \leq n \leq 1.90$ per site, driven by short-range
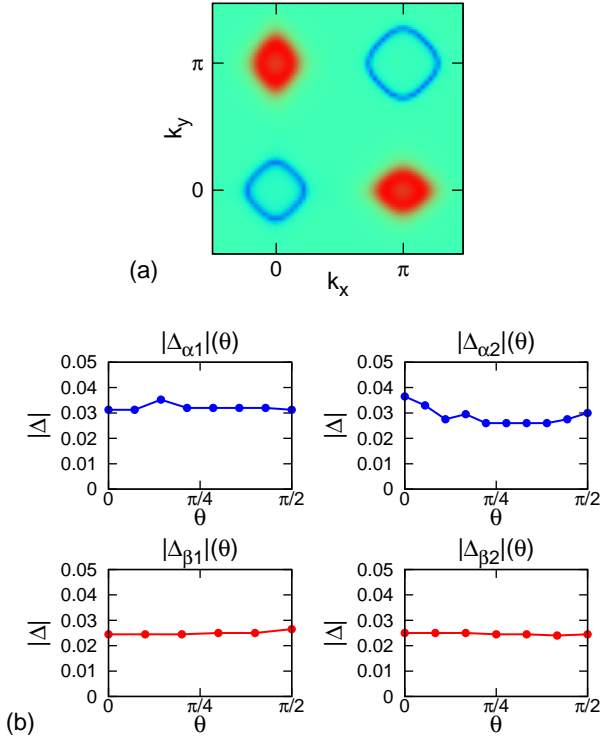
Figure 1: (Color online) (a) The renormalized Fermi surface at $T \approx 0.1T_c$ for $n = 1.88$. (b) Gap magnitude $|\Delta|$ versus angle around each FS sheet. There is an overall sign change in Δ between the α and β sheets.

spin fluctuations for certain range of coupling constants. The achieved SC states are of $s^{\pm}$-wave symmetry: fully gapped on each FS sheet with an overall sign change between the α and β sheets. To illustrate the momentum structure of the gap function, we show the results for a typical set of coupling constants $U = 1.5$, $U' = 1.2$ and $J = J' = 0.8$ with particle density $n = 1.88$ at $T = 0.001$. In this case the system exhibits a transition from the paramagnetic normal state to the SC state at $T_c = 0.0075$ and the static spin susceptibility $\chi_s(\mathbf{q}, \omega = 0)$ shows well pronounced peaks at the commensurate wave vector $\mathbf{Q}_{\mathrm{AFM}} = (0, \pi)$, $(\pi, 0)$ both in the normal and in the SC state. Note that we do not assign specific units to the parameters and quantities: The coupling constants scale with the hopping parameters and all energies scale with the SC gap magnitude while the temperatures scale with T_c. In Fig. 1 (a), we show the renormalized FS configuration obtained from the intensity projection of the Cooper-pair wave function $F(\mathbf{k}, \omega)$. Taking the small damping parameter $\delta = 0.002$ in the analytical continuation for the $T = 0.001$ solution and subtracting the gap magnitude from the spectral function $A(\omega)$ at the Fermi wave vectors $\mathbf{k}_F$ for each FS sheet, the variation in the gap magnitude on each separated FS sheet is plotted in Fig. 1 (b). Clearly in this case the gap is nearly isotropic on each pocket. The ratio $2\Delta/T_c \sim 6 - 8$ implies a strong coupling system.

IV. SHORT-RANGE SPIN FLUCTUATIONS

In this section we investigate the momentum structure of the short-range magnetic fluctuations that mediate superconductivity and make connection with the magnetic response measured in INS experiments. Our main points are as follows:

- The short-range spin fluctuations that are capable of driving the fully gapped $s^{\pm}$ superconductivity generally exhibit an anisotropy in momentum space with $\mathbf{q}$-width larger along the direction transverse to $\mathbf{Q}_{\mathrm{AFM}}$ than along the longitudinal direction. This can be understood by examining the intra-orbital scattering processes in systems away from perfect nesting.

- The momentum structure of the spin excitations exhibits the same type of anisotropy, which, in the SC state, gives rise to an elliptical shape of the spin resonance mode. Further, the resonance mode disperses with increasing energy in the pattern broadening more rapidly along the transverse than along the longitudinal direction. This anisotropic dispersion of the resonance mode associated with the intrinsic anisotropy of the mode leads to more elliptically shaped $\mathbf{q}$-image.

- The dispersion of the magnetic resonance shows an upward pattern with increasing energy in the nearly isotropic $s^{\pm}$ state with commensurate magnetic peak. But the weight of the mode decays dramatically and vanishes above the particle-hole threshold.

- In the strong coupling approach, the resonance energy is affected by the SC gap magnitude and the magnetic correlation strength.

To illustrate these points, we present the results for the magnetic susceptibility $\chi_s(\mathbf{q}, \omega)$ calculated using the typical set of parameters mentioned in the previous section followed with discussions. As Park et al.[43] show that the unfolded BZ description of the magnetic spectrum in the paramagnetic state is justified, our spin-fluctuation spectrum calculated in the BZ with 1 Fe ion is discussed below. The qualitative agreement of the calculated anisotropy with that observed in INS, in turn, suggests that the magnetic spectrum originates predominantly from the Fe-sublattice. In the following we refer to the transverse (TR) or longitudinal (LO) direction as the direction transverse or longitudinal to the corresponding AFM momentum transfer $\mathbf{Q}_{\mathrm{AFM}}$.

Results

To analyze the momentum structure of the spin fluctuations, we begin with the static spin susceptibility $\mathrm{Re}\chi_s(\mathbf{q}, \omega = 0)$. As shown in Fig. 2, besides that the
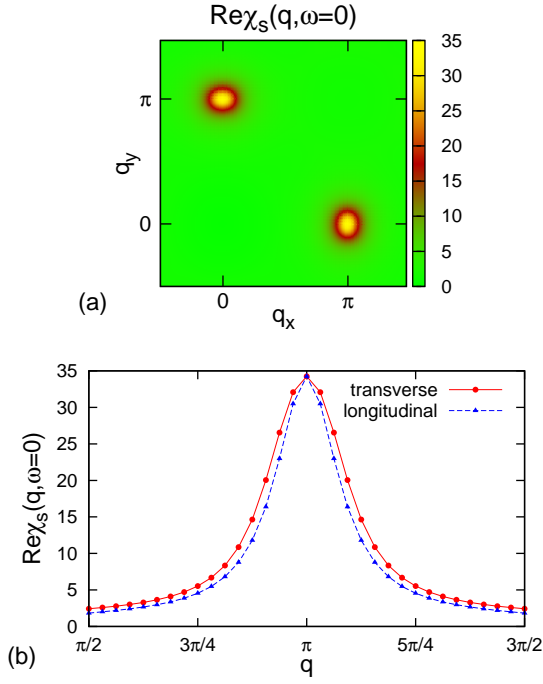
Figure 2: (Color online) The **q**-anisotropy of the static spin susceptibility. (a) is the intensity plot of $\mathrm{Re}\chi_s(\mathbf{q}, \omega = 0)$ in the momentum space and (b) shows the scans along the TR (red solid circle) and LO (blue solid triangle) direction, respectively.
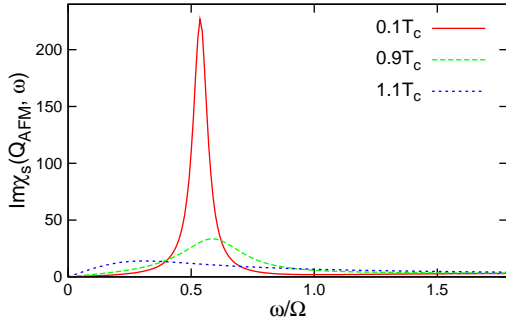

Figure 3: (Color online) Magnetic spectrum at the momentum transfer $\mathbf{Q}_{\mathrm{AFM}}$ slightly above ($T \approx 1.1T_c$) and below ($T \approx 0.9T_c$) the transition temperature T_c, as well as deep in the superconducting state ($T \approx 0.1T_c$).

static response achieves strongest enhancement at $\mathbf{Q}_{\mathrm{AFM}}$, spins are correlated spatially in an anisotropic manner with the largest span along the TR direction and smallest along the LO direction in momentum space. This results in an elliptically shaped momentum structure. Our systematic study shows that the degree of anisotropy increases with the deviation from the perfect nesting in the electronic structure. Moreover, the calculation for the temperature right above and right below the transition temperature shows that the spatial correlation does
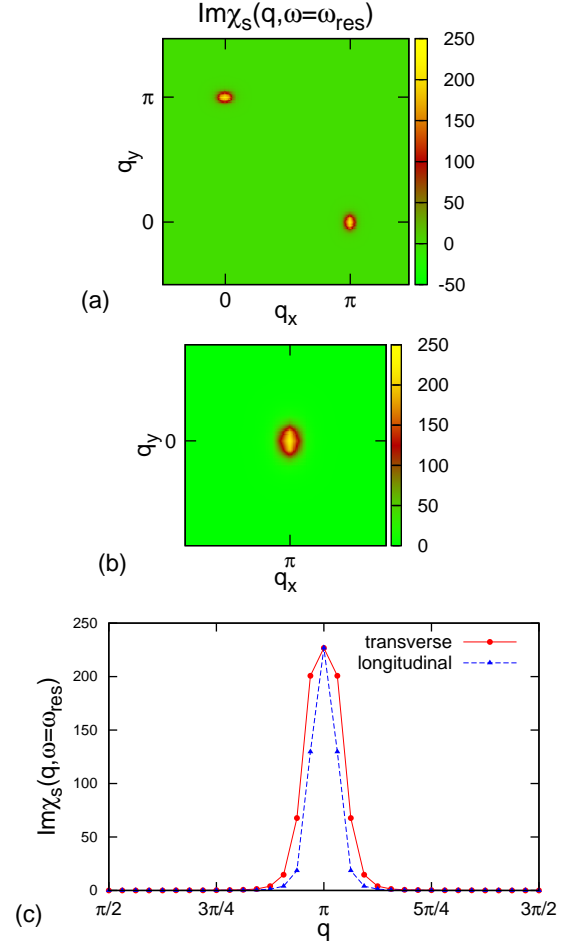

Figure 4: (Color online) The **q**-anisotropy of the spin resonance mode. (a) is the intensity plot of $\mathrm{Im}\chi_s(\mathbf{q}, \omega_{\mathrm{res}})$ at the resonance energy in the momentum space and (b) gives a zoom-in image of the resonance mode at $(\pi, 0)$. (c) shows the scans along the TR (red solid circle) and LO (blue solid triangle) direction, respectively.

not change through T_c, reflecting the fact that spin-fluctuation induced superconductivity does not modify magnetic correlation length when entering SC phase, although it is the same electrons that contribute to the magnetic and SC properties. This is in agreement with the INS observations.[27]

The imaginary part of the spin susceptibility $\mathrm{Im}\chi_s(\mathbf{q}, \omega)$ contains information on the magnetic excitations. As discussed for a sign-reversed SC gap structure, the most striking feature of the magnetic spectrum is the appearance of a resonance mode at the characteristic momentum transfer $\mathbf{Q}_{\mathrm{AFM}}$ when entering SC phase in spite of no long-range magnetic order. This sharp mode is of spin-excitonic type in our model, originated from the Stoner enhancement factor $\left[\det\left|\hat{1} - \hat{\chi}_{s,0}(\mathbf{q}, i\nu_n)\hat{U}_s\right|\right]^{-1}$.[28,29] Indeed, our calculation indicates a well-pronounced quasiparticle-like peak as
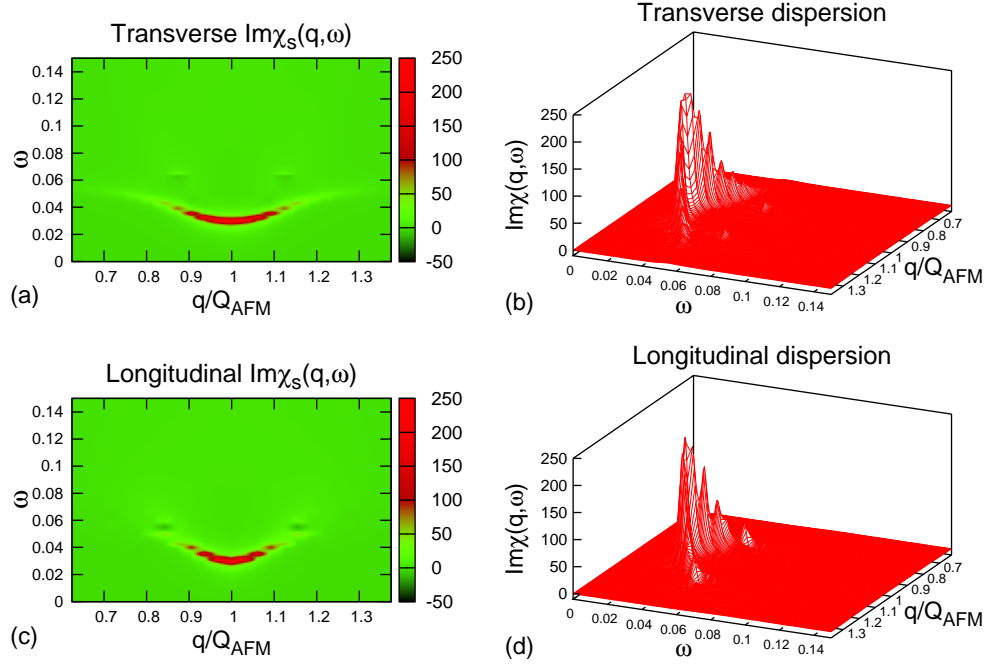
Figure 5: (Color online) The anisotropic dispersive behavior of the resonance mode along the TR and LO directions with respect to $\mathbf{Q}_{AFM}$. (a) and (c) are the intensity plot along the TR and LO direction, respectively, while (b) and (d) show the weight decay of the propagating mode.

shown in Fig. 3. In this figure, the results for the spin susceptibility $\mathrm{Im}\chi_s(\mathbf{Q}_{AFM}, \omega)$ as a function of frequency at the momentum transfer $\mathbf{Q}_{AFM}$ for temperatures $T \approx 1.1T_c$, $T \approx 0.9T_c$ and $T \approx 0.1T_c$ are presented. In the normal state the magnetic spectrum exhibits a broad continuum associated with the overdamping feature of the spin fluctuations. The transition to SC state modifies the spectrum by pushing the spectral weight to higher energy and rapidly developing a resonance mode as the temperature decreasing. The fact that this mode is made out of a particle-hole bound state in the excitonic form leads to an energy threshold taking the minimal value of sums of two gap magnitudes on any pair of FS points connected by the momentum transfer $\mathbf{Q}_{AFM}$. Here we refer to this threshold as $\Omega \equiv \min_{\mathbf{k}} \left(|\Delta_{\mathbf{k}}| + |\Delta_{\mathbf{k}+\mathbf{Q}_{AFM}}| \right)$. For the parameter set under discussion, the ratio of the resonance energy to the threshold and to the SC transition temperature are roughly $\omega_{res}/\Omega \approx 0.6$ and $\omega_{res}/k_B T_c \approx 4$, which agrees with the experimental values measured for K- and Co-doped $BaFe_2As_2$.[19,20]

Next we analyze the momentum dependence of the magnetic spectrum at the resonance frequency ω_{res}. Figure 4 shows the results for $\mathrm{Im}\chi_s(\mathbf{q}, \omega_{res})$ where a zoom-in $\mathbf{q}$-image of the mode at $(\pi, 0)$ is given in the middle. Similar to the static magnetic response, the $\mathbf{q}$-shape of the resonance mode is also elliptical with maximal broadening along the TR direction and minimal along the LO direction. This is an intrinsic anisotropy of the magnetic spectrum not only in the SC state but also existing in
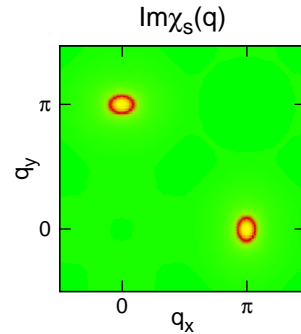

Figure 6: (Color online) The dynamical spin susceptibility averaged over a small frequency window through the resonance energy: $\frac{1}{2\Delta\omega} \int_{\omega_{res}-\Delta\omega}^{\omega_{res}+\Delta\omega} d\omega \mathrm{Im}\chi_s(\mathbf{q}, \omega)$ with $\Delta\omega = \omega_{res}/4$ here.

the normal state, which has been observed in the INS measurements.[25,27]

More interestingly, the propagation of the resonance mode also exhibits an anisotropic behavior. Figure 5 shows the dispersion of the resonance mode along the TR and LO directions at $T \approx 0.1T_c$, deep in the SC state. Two features are associated with the propagating behavior of the quasiparticle-like magnetic excitations in a fully gapped nearly isotropic $s^{\pm}$ state driven by commensurate short-range spin fluctuations: First, the resonance mode
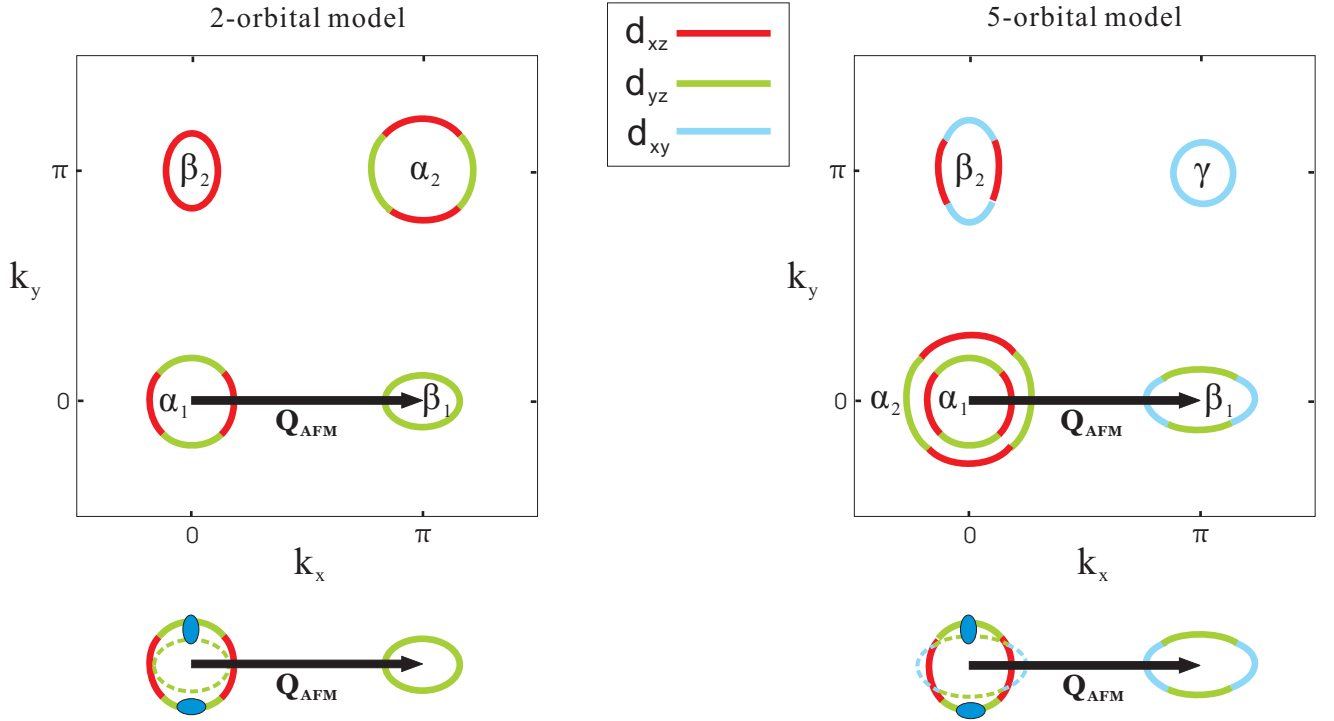
Figure 7: (Color online) Schematic illustration of the intra-orbital pair scattering processes with momentum transfer $\mathbf{Q}_{\mathrm{AFM}}$ for the 2-orbital and a more complete 5-orbital model. In the lower part, by translating $\mathbf{Q}_{\mathrm{AFM}}$, the β_1-pocket is moved to the position of the α_1-pocket. For intra-orbital, but inter-band, scattering to happen, the effective scattering vertices, depicted by the small dark-blue ellipses, should be able to cover the same orbital pieces on the two deviated FS sheets, i.e., the α_1 sheet and the shifted β_1 sheet (dashed line). One can perform similar operation for the $\alpha_1(\alpha_2)$ and $\beta_1(\beta_2)$ sheets in the 2-orbital model and for the $\alpha_1(\gamma)$ and $\beta_1(\beta_2)$ sheets in the 5-orbital model. Clearly, the transversely lengthened vertices are more capable of inducing the intra-orbital, but inter-band, pair scattering processes.

disperses with increasing energy in an anisotropic pattern broadening most rapidly along the TR rather than the LO direction as clearly seen in Fig. 5 (a) and (c), reminiscent of the anisotropic propagation of spin waves in the spin density wave state of the 122 parent compound;[44] second, the resonance mode disperses upwards in energy with dramatically decreasing weight and vanishes above the particle-hole threshold Ω as shown in Fig. 5 (b) and (d). This upward dispersion is in contrast to the downward pattern in the d-wave cuprate.[45]

The anisotropy of the dispersion relation enhances the image ellipticity of the measured magnetic response, if we consider a frequency average of the spectrum over a small window through the resonance energy, i.e., $\frac{1}{2\Delta\omega}\int_{\omega_{\mathrm{res}}-\Delta\omega}^{\omega_{\mathrm{res}}+\Delta\omega} d\omega \mathrm{Im}\chi_s(\mathbf{q},\omega)$, mimic the observation in INS. This enhanced ellipticity due to the combination of the intrinsic and dispersing anisotropy of the resonance mode is shown in Fig. 6, where we take $\Delta\omega = \omega_{\mathrm{res}}/4$.

Discussion of the spin-fluctuation anisotropy and the $s^{\pm}$ superconductivity

A systematic study of the 2- and a 3-orbital[46] models, both in hole and in electron doped regions for a variety of coupling constants, draws our attention to the connection between the momentum anisotropy of the magnetic fluctuations and the $s^{\pm}$ superconductivity. Our normal-state calculations show that different anisotropic pattern of the fluctuations occurs at different parameter sets in different model systems, either transversely or longitudinally lengthened. But the development of short-range spin fluctuations centered at $\mathbf{Q}_{\mathrm{AFM}}$ does not necessarily lead to superconductivity. For the various systems we have studied, the establishment of a stable $s^{\pm}$ state is generally associated with the transversely lengthened fluctuations. This is the characteristic momentum structure of the static correlations and of the magnetic spectra both in the normal and in the SC state. It poses a question: is superconductivity sensitive to the momentum structure of the magnetic glue?

Here we discuss how the specific momentum structure of the spin fluctuations affects the $s^{\pm}$ superconductivity in the magnetic scenario where the same electrons contribute to both the magnetic and the SC properties. We gain the insight by recognizing the important role played by the orbital weight on the FS sheets. As pointed out by Kemper et al.,[14] the dominant pairing processes involve intra-orbital scattering. The intra-orbital effective pairing interaction vertex $\Gamma_A^{cc,cc}$ is dominated by the pro-

cesses of exchanging spin-1 fluctuations as

$$\Gamma_A^{cc,cc}\left(\mathbf{k},\mathbf{k}',i\nu_n\right) \sim \frac{3}{2}\sum_{aa,bb} U_s^{cc,aa}\chi_s^{aa,bb}\left(\mathbf{k}-\mathbf{k}',i\nu_n\right)U_s^{bb,cc}$$

where a,b,c are orbital indices and $\Gamma_A^{cc,cc}$ becomes significant when the momentum transfer $\mathbf{k}-\mathbf{k}' \sim \mathbf{Q}_{\mathrm{AFM}}$. It gives rise to the intra-orbital Cooper-pair formation through

$$\Phi^{cc}(\mathbf{k},i\omega_n) = \frac{T}{N}\sum_{\mathbf{k}',\omega_n'}\Gamma_A^{cc,cc}(\mathbf{k},\mathbf{k}',i\omega_n - i\omega_n')F^{cc}(\mathbf{k}',i\omega_n')$$

which scatters a pair of c-orbital electrons on $\alpha(\beta)$ sheets to a pair of c-orbital electrons on $\beta(\alpha)$ sheets, i.e., an inter-band scattering.

A schematic demonstration of the FS configuration, with predominant iron d-orbital distribution indicated, for the current 2-orbital model and for a more complete 5-orbital model are shown in Fig. 7, which were analyzed by Graser $et\ al.$[38] and Kemper $et\ al.$[14]. To illustrate the pair scattering between two bands with the typical momentum transfer, β_1 pocket is translated by $\mathbf{Q}_{\mathrm{AFM}}$ to overlap with α_1 pocket. As the electronic structure is away from perfect nesting, the intra-orbital scattering is more supported by the transversely lengthened pairing vertices than the longitudinally lengthened ones which are depicted by the small dark-blue ellipses in the figure. One can perform the same translation for other pairs of pockets separated by $\mathbf{Q}_{\mathrm{AFM}}$ in both models and draw the same conclusion. Therefore, due to the orbital character of the microscopic electronic structure and the deviation from perfect nesting, this type of anisotropic momentum structure of short-range spin fluctuations favor the formation of $s^{\pm}$ SC state, since the intra-orbital pairing processes are made more plausible driven by transversely lengthened fluctuations.

Factors affecting the resonance energy

In the strong coupling approach, the factors affecting the resonance mode energy involve the SC gap magnitude $|\Delta|$ and the magnetic correlation length ξ.[29] Our systematic study indicates that the resonance energy ω_{res} increases with increasing gap magnitude but decreases with increasing correlation length.

V. FERMIONIC SPECTRUM

As discussed for cuprates,[28–30] the impact of the mediating bosonic modes on fermions leaves fingerprint in the fermionic spectrum, the SC spectral function, if the bosonic excitations are gapped quasiparticles such as optical phonons in the conventional superconductors. This gives rise to the kink feature in the electronic energy dispersion observed in ARPES measurements. The signature of electron-mode coupling is believed to be linked
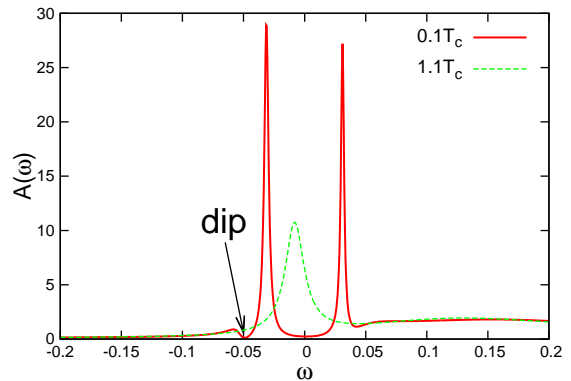

Figure 8: (Color online) The fermionic spectral function $A(\omega)$ at a $\mathbf{k}$-point on the α_1 sheet in the SC ($T \approx 0.1T_c$) state (red solid line) as well as in the normal ($T \approx 1.1T_c$) state (green dashed line). Notice the peak-dip-hump feature in the negative frequency regime when the system becomes superconducting. Comparing the SC state data with the normal state data, we see that the spectral weight is conserved.

to the pairing. If short-range spin fluctuations mediate Cooper pairs, with the emergence of the gapped quasiparticle-like spin resonance mode in the superconducting state, large fermionic decay occurs by exchange of the magnetic resonance mode in scattering processes. This leaves a dip in the electronic spectral function at the energy $\omega_{\mathrm{dip}} = |\Delta_{\mathbf{k}+\mathbf{Q}_{\mathrm{AFM}}}| + \omega_{\mathrm{res}}$ where $|\Delta_{\mathbf{k}+\mathbf{Q}_{\mathrm{AFM}}}|$ indicates the SC gap magnitude at the Fermi point connected by the AFM wave vector. Indeed, our calculation does show the dip feature in the electronic spectral function. As shown in Fig. 8, the spectral function at a $\mathbf{k}$-point on the α_1 sheet exhibits the characteristic peak-dip-hump behavior in $A_{\mathbf{k}}(\omega)$ with the dip position $\omega_{\mathrm{dip}} \approx 0.05$ to be the sum of the resonance energy $\omega_{\mathrm{res}} \approx 0.03$ and the gap magnitude $|\Delta_{\mathbf{k}+\mathbf{Q}_{\mathrm{AFM}}}| \approx 0.02$ at the point on the other band connected by $\mathbf{Q}_{\mathrm{AFM}}$. The normal state data at the same $\mathbf{k}$-point is also plotted in Fig. 8 to show the conservation of spectral weight.

VI. CONCLUSIONS

In summary, we have investigated the momentum structure of the short-range magnetic fluctuations that drive the nearly isotropic $s^{\pm}$ superconductivity using a microscopic model for the Fe-based superconductors in the self-consistent fluctuation exchange approximation. The calculated magnetic response exhibits an anisotropic feature with largest momentum span along the direction transverse to the momentum transfer $\mathbf{Q}_{\mathrm{AFM}}$, which gives rise to an elliptical image of the magnetic excitation. The calculated momentum anisotropy of the magnetic spectrum agrees with the INS measurements. An analysis on the orbital character of the electronic structure associated with the deviation from perfect nesting shows that

the transversely lengthened short-range spin fluctuations enhance intra-orbital, but inter-band, pair scattering processes that play an important role to the formation of $s^\pm$-wave superconductivity in this system. Therefore, this anisotropic momentum structure of the magnetic fluctuations favors the development of the SC phase in the magnetic scenario for the iron-based superconductors.

Our detailed study on the resonance mode in the magnetic spectrum shows that the dispersion of the mode is also anisotropic with larger broadening along the transverse than the longitudinal direction. Meanwhile, the mode propagates upwards with increasing energy in the case of nearly isotropic $s^\pm$-state and commensurate spin susceptibility, but vanishes above the particle-hole threshold.

As the feedback from the spin excitations on fermions, the spectral function exhibits the peak-dip-hump feature, which serves as one of the interpretations of the ARPES observation of the kink feature.

[1] Y. Kamihara, T. Watanabe, M. Hirano, and H. Hosono, J. Am. Chem. Soc. **130**, 3296 (2008).

[2] L. Boeri *et al.*, Phys. Rev. Lett. **101**, 026403 (2008).

[3] For example, see a recent review by D. J. Scalapino, arXiv: 1002.2413, 2010.

[4] P. Monthoux, D. Pines, and G. G. Lonzarich, Nature **450**, 1177 (2007).

[5] A. V. Chubukov, D. V. Efremov, and I. Eremin, Phys. Rev. B **78**, 134512 (2008).

[6] F. Wang, H. Zhai, Y. Ran, A. Vishwanath, and D.-H. Lee, Phys. Rev. Lett. **102**, 047005 (2009).

[7] I. I. Mazin, D. J. Singh, M. D. Johannes, and M. H. Du, Phys. Rev. Lett. **101**, 057003 (2008).

[8] K. Kuroki, S. Onari, R. Arita, H. Usui, Y. Tanaka, H. Kontani, and H. Aoki , Phys. Rev. Lett. **101**, 087004 (2008).

[9] I. I. Mazin and J. Schmalian, Physica C **469**, 614 (2009).

[10] H. Ikeda, R. Arita, and J. Kunes, Phys. Rev. B **81**, 054502 (2010).

[11] M. A. Tanatar, N. Ni, A. Thaler, S. L. Bud'ko, P. C. Canfield, and R. Prozorov, arXiv:1006.2087, 2010.

[12] F. Wang, H. Zhai, and D.-H. Lee, Phys. Rev. B **81**, 184512 (2010).

[13] R. Thomale, C. Platt, W. Hanke, and B. A. Bernevig, arXiv: 1002.3599, 2010. (unpublished)

[14] A. F. Kemper, T. A. Maier, S. Graser, H.-P. Cheng, P. J. Hirschfeld, and D. J. Scalapino, New J. Phys. **12**, 073030 (2010).

[15] T. A. Maier and D. J. Scalapino, Phys. Rev. B **78**, 020514(R) (2008).

[16] M. M. Korshunov and I. Eremin, Phys. Rev. B **78**, 140509(R) (2008).

[17] T. A. Maier, S. Graser, D. J. Scalapino, and P. Hirschfeld, Phys. Rev. B **79**, 134520 (2009).

[18] K. Seo, C. Fang, B. A. Bernevig, and J. Hu, Phys. Rev. B **79**, 235207 (2009).

[19] A. D. Christianson *et al.*, Nature (London) **456**, 930 (2008).

[20] M. D. Lumsden *et al.*, Phys. Rev. Lett. **102**, 107005 (2009).

[21] S. Chi *et al.*, Phys. Rev. Lett. **102**, 107006 (2009).

[22] S. Li *et al.*, Phys. Rev. B **79**, 174527 (2009).

[23] M. D. Lumsden *et al.*, Nature Physics **6**, 182 (2010).

[24] S. Li *et al.*, Phys. Rev. Lett. **105**, 157002 (2010).

[25] C. Lester, *et al.*, Phys. Rev. B **81**, 064505 (2010).

[26] S. O. Diallo, *et al.*, Phys. Rev. B **81**, 214407 (2010).

[27] H.-F. Li, *et al.*, Phys. Rev. B **82**, 140503(R) (2010).

[28] M. Eschrig, Adv. Phys. **55**, 47 (2006).

[29] Ar. Abanov, A. Chubukov, Phys. Rev. Lett. **83**, 1652 (1999).

[30] Ar. Abanov, A. Chubukov, and J. Schmalian, Journal of Electron Spectroscopy and Related Phenomena **117**, 129 (2001).

[31] P. Richard *et al.*, Phys. Rev. Lett. **102**, 047003 (2009).

[32] L. Wray *et al.*, Phys. Rev. B **78**, 184508 (2008).

[33] A. Koitzsch *et al.*, Phys. Rev. Lett. **102**, 167001 (2009).

[34] S. Raghu, X.-L. Qi, C.-X. Liu, D. J. Scalapino, and S.-C. Zhang, Phys. Rev. B **77**, 220503(R) (2008).

[35] R. Sknepnek, G. Samolyuk, Y.-B. Lee, and J. Schmalian, Phys. Rev. B **79**, 054511 (2009).

[36] J. Zhang, R. Sknepnek, R. M. Fernandes, and J. Schmalian, Phys. Rev. B **79**, 220502(R) (2009).

[37] K. Kuroki, H. Usui, S. Onari, R. Arita, and H. Aoki, Phys. Rev. B **79**, 224511 (2009).

[38] S. Graser, T. A. Maier, P. J. Hirschfeld, and D. J. Scalapino, New J. Phys. **11**, 025016 (2009).

[39] N. E. Bickers, D. J. Scalapino, and S. R. White, Phys. Rev. Lett. **62**, 961 (1989).

[40] C.-H. Pao and N. E. Bickers, Phys. Rev. Lett. **72**, 1870 (1994).

[41] P. Monthoux and D. J. Scalapino, Phys. Rev. Lett. **72**, 1874 (1994).

[42] T. Takimoto, T. Hotta, and K. Ueda, Phys. Rev. B **69**, 104504 (2004).

[43] J. T. Park, *et al.*, Phys. Rev. B **82**, 134503 (2010).

[44] K. Matan, R. Morinaga, K. Iida, and T. J. Sato, Phys. Rev. B **79**, 054526 (2009).

[45] I. Eremin, D. K. Morr, A. V. Chubukov, K. H. Bennemann, and M. R. Norman, Phys. Rev. Lett. **94**, 147001 (2005).

[46] M. Daghofer, A. Nicholson, A. Moreo, and E. Dagotto, Phys. Rev. B **81**, 014511 (2010).